

Effect of the electron beam modulation on the sub-THz generation in the vircator with the field-emission cathode

S. A. Kurkin^{1,2†}, A. A. Koronovskii^{1,2}
and A. E. Hramov^{1,2}

¹Saratov State University, Astrakhanskaya Street, 83, Saratov, 410012, Russia

²Saratov State Technical University, Politechnicheskaya Street, 77, Saratov, 410054, Russia

(Received 17 December 2014; revised 17 February 2015; accepted 18 February 2015;
first published online 17 March 2015)

In this paper, we focus on the numerical investigation of the vircator with a controlling emission from a field-emission cathode. The external harmonic signal is added to the accelerating electric field in the beam formation region and effects on the beam emission process leading to the electron emission modulation. As a consequence, the beam is injected into the drift chamber of the vircator being density-modulated. The strong influence of the modulation parameters (modulation depth and frequency) on the characteristics of virtual cathode oscillations has been discovered. We have shown that the tuning of the modulation frequency to the harmonics of the basic frequency of virtual cathode oscillations leads to the considerable power increase of its higher harmonics in the output spectrum.

1. Introduction

The microwave generators with a virtual cathode (VC) – virtual cathode oscillators (VCOs, vircators) – are the perspective devices of vacuum and plasma high-power microwave electronics for the generation of the impulses of microwave radiation due to their high output power, a simple construction (particularly, vircators can operate without the external focusing magnetic field), the possibility of a simple frequency tuning and regime switching (tunability) (Burkhart et al. 1985; Sullivan et al. 1987; Hoerberling and Fazio 1992; Gold and Nusinovich 1997; Dubinov and Selemir 2002; Benford et al. 2007; Liu et al. 2008; Hramov et al. 2012; Clements et al. 2013; Kurkin et al. 2013). The operation of VCOs (vircators, virtodes, reflex triodes, etc.) is based on the formation of the VC in the electron beam with overcritical current (Mahaffey et al. 1977; Sullivan et al. 1987; Kostov et al. 1993, 1999; Benford et al. 2007; Hramov et al. 2010; Verma et al. 2014). At the present time the increase of the efficiency, the power and the generation frequency (the advancement to the sub-THz range) of a vircator and the development of the methods for the control of its generation characteristics are the actual problems of a modern plasma physics and high-power microwave electronics. Such problems are closely associated with the possibility of the various applications of vircators (the problems of electromagnetic compatibility, technological processes, impulse radiolocation, etc.) (Sullivan et al. 1987; Dubinov and Selemir 2002; Benford et al. 2007).

† Email address for correspondence: kurkinsa@gmail.com

The early researches of the vircators with external resonance systems have shown (Gadetskii et al. 1993; Jiang et al. 2004; Shao et al. 2005; Kovalchuk et al. 2010; Shlapakovski et al. 2012; Yang et al. 2013) that the effective approach for the improvement of vircator characteristics is the introduction of the velocity (Anfinogentov and Hramov 2001; Jiang et al. 2004; Shlapakovski et al. 2012; Yang et al. 2013; Phrolov et al. 2014) or density (Gadetskii et al. 1993; Yang et al. 2013) modulation of the electron beam in such generators. The use of the electron source with the emission modulation is the effective method for the realization of the deep density modulation of a beam in the interaction space by means of a relatively low-power external signals (Dzbanovskii et al. 2005).

At the present time, the field-emission cathodes (Spindt array, Latham emitter et al.) are widely applied in high-power microwave electronics and, particularly, in the design of relativistic vircators due to their undoubted advantages (Rozhnev et al. 2002; Benford et al. 2007; Krasik et al. 2009; Shlapakovski et al. 2009). So, the investigation of the influence of the emission modulation and its parameters on the generation characteristics of the relativistic vircator with the field-emission cathode from the point of view of the possibility of the vircator characteristics (efficiency, output microwave power, generation frequency, tunability) improvement is the actual problem of high-power microwave electronics. The emission modulation in the system with the field-emission cathode may be realized by means of the addition of alternating modulating voltage to the accelerating one in the region of beam formation (electron gun) (Dzbanovskii et al. 2005).

In this paper, we show for the first time the results of the numerical study of the modulation parameters influence on the oscillations characteristics of the VC in the weakly relativistic vircator (Kalinin et al. 2005; Gursharn and Shashank 2008; Filatov et al. 2009; Kurkin and Hramov 2009; Kurkin et al. 2011) with the controlling field-emission electron gun within specially developed 2.5D numerical model.

2. General formalism

Let us consider the model under study (see Fig. 1). It consists of the closed finite-length equipotential cylindrical waveguide region 1 of the length L and the radius R (the interaction space of an electron beam or drift space) with the transparent grid electrodes 2 and 3 at the both ends (Hramov et al. 2010). An axially-symmetrical density-modulated solid electron beam 4 with the current $I(t)$ and the radius R_b is injected at the velocity v_0 through the left (entrance) electrode and then may leave the system through the right (exit) electrode or through the side wall of the interaction space. As we consider the field-emission gun with the emission modulation, the time dependence of beam current density $J(t)$ at the entrance plane of the model is defined by the Fowler–Nordheim law where the accelerating electric field \tilde{E} consists of a constant part and the modulating addition that varies with time harmonically (Stern et al. 1929; Dzbanovskii et al. 2005; Forbes 2008):

$$J(t) = a\tilde{E}(t)^2 \exp\left(\frac{-b\varphi_e^{3/2}}{\tilde{E}(t)}\right). \quad (2.1)$$

Here φ_e is the work function from the cathode, a and b are determined by the geometry of the model and the work function (we suppose that the material of the cathode is molybdenum). The emission of electron beam into the system occurs from the array of elementary emitters that corresponds to the Spindt-like cathode. The instantaneous current of the beam is determined as $I(t) = J(t) * S_{ef}$, where S_{ef} is

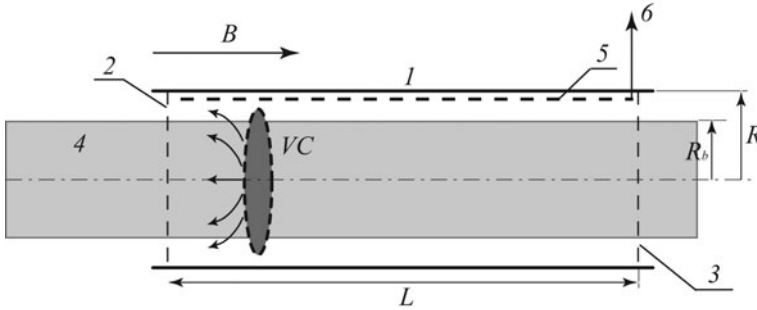


FIGURE 1. The scheme of the investigated vircator model. Here 1 is the cylindrical drift space, 2 and 3 are the entrance and the exit transparent grid electrodes respectively, 4 is the density-modulated solid electron beam, 5 is the broadband helical slow-wave system with the absorbing output insert 6. B is the external uniform focusing magnetic field, VC denotes schematically the VC area reflected part of electron beam back to the injection plane (anode).

the total area of all microemitters. The plasma effects are not considered within the framework of this paper.

The external uniform focusing magnetic field with induction B is applied along the longitudinal axis of the waveguide. The power of VC oscillations in the model is supposed to extract via a broadband helical slow-wave system 5 loaded on the absorbing output insert 6 (Kalinin et al. 2005; Hramov et al. 2010; Kurkin et al. 2011).

We have considered the time-dependent 2.5D numerical model in which the dynamics of the electron beam in the interaction space is described by the self-consistent set of Vlasov and Poisson equations (Birdsall and Langdon 2005; Antonsen et al. 1999). The Vlasov kinetic equation for the electron beam motion analysis is solved numerically by the particle-in-cell (PIC) method (Birdsall and Langdon 2005). The potential distribution in the interaction space may thus be obtained easily by numerical solving the Poisson's equation in cylindrical geometry (Birdsall and Langdon 1985).

The equations describing the dynamics of the considered model are formulated in terms of the dimensionless variables of the potential φ , the space charge field E , the induction of the external magnetic field B , the electron density ρ , the electron velocity v and impulse P , the spatial coordinates z and r , the time t and the frequency f :

$$\begin{aligned} \varphi' &= \frac{v_0^2}{\eta_0} \varphi, & E' &= \frac{v_0^2}{L\eta_0} E, & B' &= \frac{v_0}{L\eta_0} B, & \rho' &= \rho_0 \rho, \\ v' &= v_0 v, & P' &= m_e v_0 P, & z' &= Lz, & r' &= Lr, & t' &= \frac{L}{v_0} t, & f' &= \frac{v_0}{L} f. \end{aligned} \quad (2.2)$$

Here the primes mean dimensional values, $\eta_0 = e/m_e$ is the specific charge of electron, v_0 and ρ_0 are the longitudinal velocity and the space charge density of the electron beam at the entrance, respectively, and L is the length of the interaction space.

In cylindrical geometry, the particles that model the beam space charge dynamics have the form of charged rings. In terms of dimensionless values (2.2) the equations of motion in cylindrical coordinates for each charged particle are written as

$$\frac{dP_{ri}}{dt} - \gamma(z_i, \theta_i, r_i) r_i \left(\frac{d\theta_i}{dt} \right)^2 = -E_r - r_i B_z \frac{d\theta_i}{dt}, \quad (2.3)$$

$$\frac{dP_{\theta i}}{dt} + \gamma(z_i, \theta_i, r_i) \frac{dr_i}{dt} \frac{d\theta_i}{dt} = B_z \frac{dr_i}{dt}, \quad (2.4)$$

$$\frac{dP_{zi}}{dt} = -E_z, \quad i = 1, \dots, N_0, \quad (2.5)$$

where

$$\gamma(z_i, \theta_i, r_i) = \left(1 - \beta_0^2 \left[\left(\frac{dr_i}{dt} \right)^2 + \left(r_i \frac{d\theta_i}{dt} \right)^2 + \left(\frac{dz_i}{dt} \right)^2 \right] \right)^{-1/2}. \quad (2.6)$$

Here, z_i , r_i , and θ_i are the longitudinal, radial, and azimuthal coordinates of the charged particles, $P_{zi} = \gamma z_i$, $P_{ri} = \gamma r_i \dot{\theta}_i$, $P_{\theta i} = \gamma r_i \dot{\theta}_i$ are the longitudinal, radial, and azimuthal components of the particles impulses, E_z and E_r are the longitudinal and radial electric field components, $\beta_0 = v_0/c$, where v_0 is the initial velocity of the electron beam and c is the light speed. The subscript i denotes the number of particle and N_0 is the full number of charged particles using in the simulation.

The potential distribution in the interaction space is calculated self-consistently by means of Poisson's equation

$$\frac{1}{r} \frac{d\varphi}{dr} + \frac{d^2\varphi}{dr^2} + \frac{d^2\varphi}{dz^2} = \alpha^2 \rho, \quad (2.7)$$

where

$$\alpha = L \left(\frac{|\rho_0|}{V_0 \epsilon_0} \right)^{1/2} \quad (2.8)$$

is the dimensionless control parameter which depends on beam current as $\alpha \sim \sqrt{I}$ and is proportional to the length of the interaction space as $\alpha \sim L$. Here V_0 is the constant part of the accelerating potential. Poisson's equation (2.7) is solved with the following boundary conditions

$$\varphi(z = 0, r) = 0, \quad \varphi(z = 1, r) = 0, \quad \varphi(z, r = R) = 0, \quad (2.9)$$

$$\left. \frac{d\varphi}{dr} \right|_{r=0} = 0. \quad (2.10)$$

Condition (2.9) implies that the potential of the conducting cylindrical surface 1–3 of the radius R bounding the interaction space equals to zero. Condition (2.10) means that there is no radial component of the electric field at the symmetry axis $r = 0$ due to the axial symmetry of the drift chamber of vircator.

The equations of motion (2.3)–(2.5) are integrated numerically for each particle by the second-order leap-frog method (Birdsall and Langdon 1985). Poisson's equation (2.7) is solved at each time step on the two-dimensional mesh in cylindrical coordinates. Output microwave signal extracted by the broadband slow-wave system is simulated by means of the conventional equivalent circuit method (Morey and Birdsall 1990; Egorov et al. 2006).

For the simulation of the beam with the time-dependent initial beam current $I(t)$ the each following part of charged particles is injected in the system not at regular time intervals but the each time moment of particles injection is determined in accordance with the law of the current change with time. In other words, the injection frequency varies with time according to the change of the current $I(t)$.

The basic control parameters of the considered system are the depth of current modulation $D = \frac{I_{\max} - I_{\min}}{I_{\max}} * 100\%$ (I_{\max} and I_{\min} are the maximal and minimal values of the time dependency of beam current $I(t)$ at the entrance plane, respectively); the

dimensionless frequency of modulation f_m , and the value of current supercriticality $A = I/I_{cr}$ that determines the excess of a beam current I over the critical value I_{cr} . The value I_{cr} is the minimum current (the so-called space-charge limiting current) for which the VC formation in electron beam is observed.

Note also, that in the present paper, we consider the nonlinear dynamics of weakly relativistic electron beams. The mathematical model where the self-consistent space charge field is obtained from Poisson's equation does not provide a correct analysis of the system with electron beams with the normalized velocity of $\beta_0 = v_0/c \gtrsim 0.5$, since it does not take into account the self-magnetic field of the electron beam and the associated beam pinching effects (Gursharn and Shashank 2008). However, for the weakly relativistic beams ($\beta_0 \lesssim 0.5$) the role of the self-magnetic fields of the electron beam is vanishingly small and may be neglected. Actually, the electron focusing force of the self-magnetic field of the electron beam, $F_{r1} = \mu_0 e \rho v_0^2 r / (2\pi R_b^2) \sim 10^{-4}$ N, is significantly less than the focusing force $F_{r2} = r B_0 \dot{\theta}_i \sim 10^4$ N determined by the external magnetic field and the gyrotory electron velocity.

3. The results of numerical investigation

Using the developed numerical model, we have analyzed the influence of the emission modulation on the virtual cathode oscillations in the vircator with the controlling field-emission electron gun. First of all, let us consider the process of the propagation of density-modulated beam in the system. Figure 2 demonstrates the space-time diagrams (t, z) of the density-modulated electron beam in the vircator and the time dependencies of the radially averaged space charge oscillations $\rho(t)$ at the VC area in the cases of subcritical (a), overcritical (b) and strongly overcritical (c) currents. In the first case one may observe the formation and propagation of the electron bunches (corresponding to thickening of the trajectories the space-time diagrams) along the longitudinal axis due to the density premodulation of the beam injected into the drift space. The minima at $\rho(t)$ dependency correspond to the time moments when a bunch reaches the VC area. The constancy of the trajectories slopes at the space-time diagram indicates that the space-charge forces don't influence practically on the electrons motion in the system, and they move at an approximately constant speed in this case of a low beam current. The time dependency $\rho(t)$ demonstrates periodic behavior with period determining by the modulation one.

With the growth of the beam current when the system switches to the overcritical regime, the pattern of the space-time diagram changes qualitatively (Fig. 2b). Against the background of the electron beam density modulation the VC is formed in the system and reflects periodically the part of the beam back to the entrance plane. The VC is maximally developed when the beam density in its area is near the maximal value and may disappear (on certain parameters of emission modulation) when it reaches minimum. Also Fig. 2b demonstrates, that a part of the reflected from the VC electrons remains in the system during a few VC oscillations periods. This electrons influence on the VC formation process and provide the additional internal electron feedback loop. The time dependency of the space charge oscillations $\rho(t)$ at the VC area are the double-period in this case, that is the consequence of the presence of two character time scales in the system: the VC oscillations period and the modulation period. Nevertheless, modulation process prevails over the VC oscillations.

With the further growth of the beam current the strongly overcritical regime is established in the system (Fig. 2(c)). VC is formed close to the entrance plane in this case, and not only when a bunch of density-modulated electron beam reaches

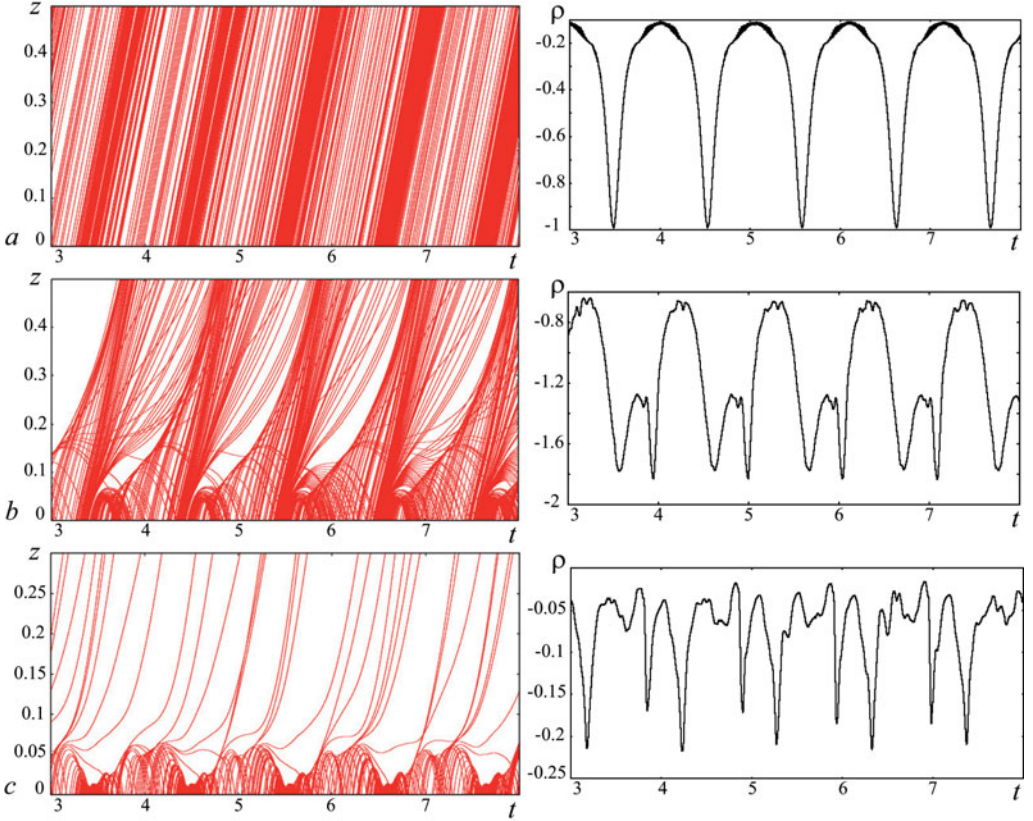


FIGURE 2. The space-time diagrams of the electrons from the middle layer of electron beam in the dimensionless coordinates (t, z) and the corresponding time dependencies of the radially averaged space charge oscillations $\rho(t)$ at the VC area for (a) $A = 0.42$, $D = 95\%$ (subcritical regime), (b) $A = 2.1$, $D = 90\%$ (overcritical regime), and (c) $A = 4.9$, $D = 95\%$ (strongly overcritical regime); $B = 20$, $f_m = 1$.

the VC area but when the electron beam density is in phase of minimum in this area, that is the consequence of a strong space charge forces. So, the quantity of the reflected particles is larger and the VC dynamics is more complex in the case of strong overcriticality. The both processes (i.e. modulation and VC oscillations) play a significant role in the development of system dynamics in this case. The consequence is a complex (quasiperiodic) behavior of the $\rho(t)$ dependency.

Let us consider the results of the numerical simulation on the investigation of the influence of emission modulation parameters on the generation characteristics of the vircator model. When the modulation is deep ($D > 80\%$) and the current supercriticality is relatively small ($1 < A < 3$), the spectral composition of output radiation is defined by the frequency of modulating harmonic signal and contains the first, the second, and the third harmonics of this frequency. For example, when $A = 2.1$, $D = 100\%$, $f_m = 1.9$ (Fig. 3(a)) the output spectrum contains components at frequencies about 1.9, 3.8 and 5.7, and the ratio of their amplitudes is following: 6 : 3 : 1; the frequency of VC free oscillations f_{VC} (in the system without emission modulation) in this case is about 2.6. Also sideband components of the harmonics of

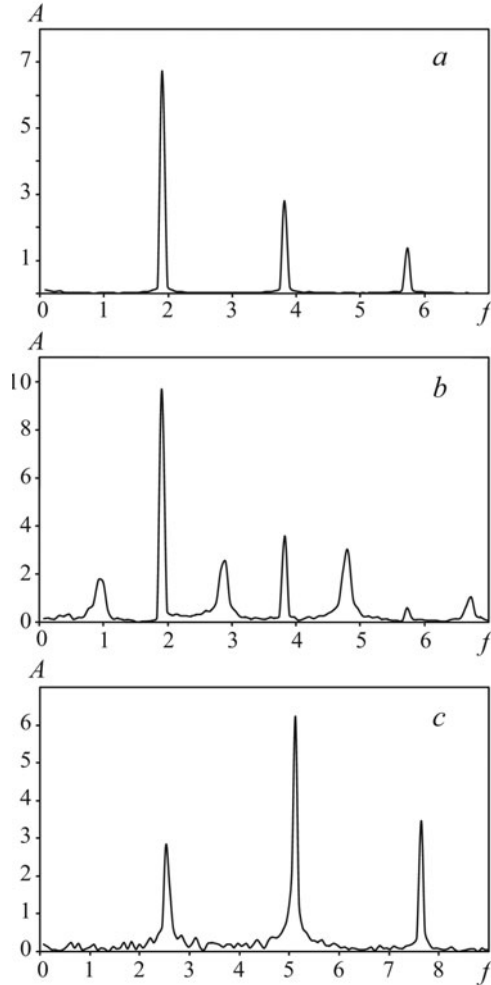


FIGURE 3. The amplitude spectra of the output signal of the considered vircator model with the emission modulation for (a) $A = 2.1$, $D = 100\%$, $f_m = 1.9$; (b) $A = 6.3$, $D = 100\%$, $f_m = 0.95$; and (c) $A = 4.9$, $D = 80\%$, $f_m = 2.55$; $B = 20$.

the modulating signal frequency and free VC oscillations frequency may be present in the spectrum at certain parameters, but their amplitudes are low.

So, the breaking (full or partial) of VC formation mechanisms occurs in the model in the case of the deep current modulation ($D > 80\%$) and relatively small values of current supercriticality parameter A (see also Fig. 2(b)). Electron beam is injected as the sequence of electron bunches in this case with the repetition frequency and density being determined by the parameters of the modulating signal. It leads to the decrease of space charge density in the interaction space and the VC is not formed in the system. This effect is most pronounced for large periods of the modulating harmonic signal. In this case, the space charge decreases significantly during the negative phase of the modulating signal when the injection of new electrons becomes less, so the critical space charge density necessary for the formation of VC is not achieved. At the same time, the modulated electron beam (the sequence of electron bunches) excites efficiently the output electrodynamic system of the vircator (e.g. spiral

slow-wave structure) at the modulation frequency and its harmonics. In other words, the external modulating signal imposes its dynamics and breaks the VC formation mechanism that is reflected on the spectrum of output microwave radiation.

VC arises in the system with the deep emission modulation again with the further increase of current supercriticality (see also Fig. 2(c)). So, when $A > 3$ and $D = 100\%$ the form of output spectrum is changed qualitatively in comparison with the previous case (see Fig. 3(b)). Besides the components multiple of the modulation frequency, the harmonics of free VC oscillations and their sideband components appear in the spectrum. Note that the amplitudes of this sideband components are maximal in most cases that indicates the strongly nonlinear regime of the system operation. So, when $A = 6.4$, $D = 100\%$, $f_m = 0.95$ the spectrum of output radiation (Fig. 3(b)) contains the following components: at frequency 0.95 with dimensionless amplitude 2 corresponding to the modulation frequency, at frequency 2.78 with amplitude 2.5 that corresponds to the free VC oscillations and the component at frequency 1.86 with amplitude 9.7 that is the sideband component of the modulation and free VC frequencies. Also, the output spectrum contains its second harmonic $f_m = 3.7$ with amplitude 3.6. One can see that the highest energy (about 50%) is concentrated in the sideband spectral component $f_m = 1.86$, the remaining part of energy is almost uniformly distributed between other spectral components. Thus, the complex interaction of the VC oscillations (with basic frequency proportional to the plasma frequency (Sullivan et al. 1987; Koronovskii and Hramov 2002; Benford et al. 2007)) and the electron bunches dynamics with the repetition rate determined by the modulation frequency occurs in the vircator system with the deep emission modulation and the high-current supercriticality. It leads to the appearance of the intense sideband components in the spectrum of vircator output radiation.

Let us note especially the situation of the deep current modulation $D > 80\%$ with the frequency equal to the f_{VC} . The output signal spectrum is essentially simplified in this case and consists the first, second, and third harmonics of this frequency which concentrate more than 90% of overall energy. The physical reason of this result is that the electron bunches of the modulated electron beam come to the VC area in the phase with its oscillations. The generation efficiency in this regime increases in comparison with the case of VC free oscillations.

Let us consider the results of the investigation of the vircator system with the emission modulation for less values of the modulation depth ($50\% < D < 80\%$) and average values of the current supercriticality ($1 < A < 5$). In this case, when the modulation frequency is not multiple of f_{VC} the output spectrum is similar to the discussed above case of high supercriticality and modulation depth (see Fig. 3(b)). The most interesting situation is observed in the system when the modulation frequency is tuned on the harmonic of the free VC oscillations. The significant increase of the higher harmonics amplitudes of f_{VC} occurs in the output microwave signal spectrum, while the first harmonic decreases for such system parameters. So, when $A = 4.9$, $D = 100\%$, $f_m = f_{VC} = 2.55$ (see Fig. 3(c)) the amplitude of the third harmonic at frequency $f = 7.65$ increases by two times, the second harmonic doesn't change practically and the first one decreases by two times approximately in comparison with the case of the modulation absence. Thus, energy is transferred from lower to higher harmonics. Note, it is possible to obtain the rise of power of even higher spectral components multiple of the free VC oscillations frequency f_{VC} by tuning the modulation frequency to the higher harmonics of f_{VC} . This regime of the vircator operation is rather attractive for the multiple increase of its generation frequency,

L , mm	R , mm	R_b , mm	J_0 , kA/cm ²	B , T	f_m , GHz	The frequencies of the two most intense spectral components, GHz
30	7.5	3.25	0.025	0.1	2.3	4.6; 6.9
10	2.5	1.25	0.22	0.3	6.9	13.8; 20.7
5	1.25	0.625	0.9	0.6	13.8	27.5; 41.3
3	0.75	0.375	2.5	1	23	46; 69
2	0.5	0.25	5.6	1.5	34.4	68.9; 103.2
0.5	0.125	0.0625	89	6.14	138	276; 414

TABLE 1. Estimations of the dimensional values of generation frequencies of vircators for different character parameters; here L is the length of the vircator model, R – its radius, R_b – the beam radius, J_0 – the peak current density, f_m – the modulation frequency, the modulation depth $D = 80\%$, the current supercriticality $A = 2.1$, the initial beam velocity $\beta = v_0/c = 0.1$.

in particular, for the creation of the modification of generator on VC – frequency multiplier vircator.

From the physical point of view, the initial premodulation of electron beam at the frequency multiple of the free VC oscillations frequency f_{VC} promotes its more effective formation, because the new ‘portions’ of space charge in the form of electron bunches reach the VC area when it is in the phase of charge accumulation. Hence, the beam bunching in the VC area is significantly improved and the harmonics of space charge oscillations rise considerably. The decrease of the modulation depth allows to inject current into the system sufficient for the formation and maintenance of VC. It is known, that VC usually demonstrates complex relaxation oscillations with spectrum rich in higher harmonics (Kurkin et al. 2014), so the modulation of beam at the frequency multiple of f_{VC} may lead to the increase of the amplitude of other harmonic, that we have seen in Fig. 3(c).

The Table 1 demonstrates some estimations of the dimensional values of generation frequencies for the different character parameters of vircator with the emission modulation operating in the regime with the developed higher harmonics. Suppose, that the length of the vircator model $L = 3$ mm, the radius $R = 0.75$ mm, the beam radius $R_b = 0.375$ mm, the initial beam velocity $\beta = v_0/c = 0.1$, the peak current density 2.5 kA cm^{-2} , the modulation depth $D = 80\%$, and frequency $f_m = 23$ GHz, the external magnetic field induction $B = 1$ T. Such system parameters correspond to the regime shown in Fig. 3c and the output spectrum in this regime is characterized by the intense second and third harmonics at the frequencies 46 GHz and 69 GHz, respectively.

The table shows that the vircator with the emission modulation working at the second or third harmonic of the VC free oscillations frequency may be considered as a prospective source of electromagnetic radiation in the C-, X-, Ku-, K-, V- or W-band ranges. Its operating frequency is correspondingly in 2 or 3 times higher than the frequency of vircator without emission modulation. It’s important to note that when the length of the vircator is less than 5 mm, it may be considered as the micrometer (in dimensions) generator of sub-THz radiation (Siegel et al. 2001; Nation et al. 2014). Due to its small dimensions, a number of such generators may be connected into an array (see, for example, (Woo et al. 1989; Hendricks et al. 1990; Sze et al. 1990; Dubinov et al. 2000; Dubinov and Selemir 2002; Filatov et al. 2006; Moskalenko et al. 2013)) for the significant increase of integral output power.

4. Conclusion

We have discovered the strong influence of the emission modulation parameters in the vircator on the oscillation characteristics of the beam with a VC. We have shown that the tuning of the modulation frequency to a higher harmonic of the free virtual cathode oscillations frequency allows to increase considerably the power of the higher harmonics in the output spectrum. In particular, such regime of the vircator operation is prospective for the multiple increase of its generation frequency (for the creation of frequency multiplier vircator) and, as the estimations have shown, for the advancement of vircator to the sub-THz range.

Acknowledgement

This work has been supported by the Russian Science Foundation (grant 14–12–00222). A.E.H. thanks also the Ministry of Education and Science of Russian Federation (individual grant 931).

REFERENCES

- Anfinogentov, V. G. and Hramov, A. E. 2001 Oscillation conditions of the vircator klystron with external delayed feedback: a computer simulation. *Commun. Technol. Electron.* **46**(5), 546–549.
- Antonsen, T. M., Mondelli, A. A., Levush, B., Verboncoeur, J. P. and Birdsall, C. K. 1999 Advances in modelling and simulation of vacuum electron devices. *Proc. IEEE* **87**(5), 804–839.
- Benford, J., Swegle, J. A. and Schamiloglu, E. 2007 *High Power Microwaves*. Boca Raton: CRC Press, Taylor and Francis.
- Birdsall, C. K. and Langdon, A. B. 1985 *Plasma Physics, Via Computer Simulation*. NY: McGraw-Hill.
- Birdsall, C. K. and Langdon, A. B. 2005 *Plasma Physics Via Computer Simulation*. NY: Taylor and Francis Group.
- Burkhart, S. C., Scarpetty, R. D. and Lundberg, R. L. 1985 A virtual cathode reflex triode for high power microwave generation. *J. Appl. Phys.* **58**(1), 28.
- Clements, K. R., Curry, R. D., Druce, R., Carter, W., Kovac, M., Benford, J. and McDonald, K. 2013 Design and operation of a dual vircator hpm source. *IEEE Trans. Dielectr. Electr. Insul.* **20**(4), 1085–1092.
- Dubinov, A. E. and Selemir, V. D. 2002 Electronic devices with virtual cathodes (review). *J. Commun. Technol. Electron.* **47**(6), 575.
- Dubinov, A. E., Selemir, V. D. and Tsarev, A. V. 2000 Phased antenna arrays based on vircators: Numerical experiments. *Radiophys. Quantum Electron.* **43**(8), 637–642.
- Dzbanovskii, N. N., Minakov, P. V., Pilevskii, A. A., Rakhimov, A. T., Seleznev, B. V., Suetin, N. V. and Yurev, A. Yu. 2005 High-current electron gun with a field-emission cathode and diamond grid. *Tech. Phys.* **50**(10), 1360.
- Egorov, E. N., Kalinin, Yu. A., Koronovskii, A. A., Hramov, A. E. and Morozov, M. Yu. 2006 Microwave generation power in a nonrelativistic electron beam with virtual cathode in a retarding electric field. *Tech. Phys. Lett.* **32**(5), 402–405.
- Filatov, R. A., Hramov, A. E., Bliokh, Y. P., Koronovskii, A. A. and Felsteiner, J. 2009 Influence of background gas ionization on oscillations in a virtual cathode with a retarding potential. *Phys. Plasmas* **16**(3), 033 106.
- Filatov, R. A., Hramov, A. E. and Koronovskii, A. A. 2006 Chaotic synchronization in coupled spatially extended beam-plasma systems. *Phys. Lett. A* **358**, 301–308.
- Forbes, R. G. 2008 Physics of generalized Fowler-Nordheim-type equations. *J. Vac. Sci. Technol. B* **26**(2), 788.
- Gadetskii, N. N., Magda, I. I., Naisteter, S. I., Prokopenko, Yu.V. and Tchumakov, V. I. 1993 The virtode: a generator using supercritical reb current with controlled feedback. *Plasma Phys. Rep.* **19**, 273.
- Gold, S. H. and Nusinovich, G. S. 1997 Review of high-power microwave source research. *Rev. Sci. Instrum.* **68**(11), 3945–3974.

- Singh, G. and Chaturvedi, S. 2008 Secondary virtual-cathode formation in a low-voltage vircator: pic simulations. *IEEE Trans. Plasma Sci.* **36**(3), 694–700.
- Hendricks, K. J., Adler, R. and Noggle, R. C. 1990 Experimental results of phase locking two virtual cathode oscillators. *J. Appl. Phys.* **68**(2), 820–828.
- Hoerberling, R. F. and Fazio, M. V. 1992 Advances in virtual cathode microwave sources. *IEEE Trans. Electromagn. Compat.* **34**(3), 252–258.
- Hramov, A. E., Koronovskii, A. A. and Kurkin, S. A. 2010 Numerical study of chaotic oscillations in the electron beam with virtual cathode in the external non-uniform magnetic fields. *Phys. Lett. A* **374**, 3057–3066.
- Hramov, A. E., Koronovsky, A. A., Kurkin, S. A. and Rempen, I. S. 2011 Chaotic oscillations in electron beam with virtual cathode in external magnetic field. *Int. J. Electron.* **98**(11), 1549–1564.
- Hramov, A. E., Kurkin, S. A., Koronovskii, A. A. and Filatova, A. E. 2012 Effect of self-magnetic fields on the nonlinear dynamics of relativistic electron beam with virtual cathode. *Phys. Plasmas* **19**(11), 112101.
- Jiang, W., Shimada, N., Prasad, S. D. and Yatsui, K. 2004 Experimental and simulation studies of new configuration of virtual cathode oscillator. *IEEE Trans. Plasma Sci.* **32**(1), 54–59.
- Kalinin, Yu. A., Koronovskii, A. A., Hramov, A. E., Egorov, E. N. and Filatov, R. A. 2005 Experimental and theoretical investigations of stochastic oscillatory phenomena in a nonrelativistic electron beam with a virtual cathode. *Plasma Phys. Rep.* **31**(11), 938–952.
- Koronovskii, A. A. and Hramov, A. E. 2002 Wavelet bicoherence analysis as a method for investigating coherent structures in an electron beam with an overcritical current. *Plasma Phys. Rep.* **28**(8), 666.
- Kostov, K. G., Nikolov, N. A. and Spassov, V. A. 1993 Excitation of transverse electric modes in axially extracted virtual cathode oscillator. *Electron. Lett.* **29**(12), 1069–1070.
- Kostov, K. G., Yovchev, I. G. and Nikolov, N. A. 1999 Numerical investigation of microwave generation in foilless diode vircator. *Electron. Lett.* **35**(19), 1647–1648.
- Kovalchuk, B. M., Polevin, S. D., Tsygankov, R. V. and Zherlitsyn, A. A. 2010 S-band coaxial vircator with electron beam premodulation based on compact linear transformer driver. *IEEE Trans. Plasma Sci.* **38**(10), 2819–2824.
- Krasik, Y. E., Yarmolich, D., Gleizer, J. Z., Vekselman, V., Hadas, Y., Gurovich, Tz. V. and Felsteiner, J. 2009 Pulsed plasma electron sources. *Phys. Plasmas* **16**(5), 057103.
- Kurkin, S. A., Badarin, A. A., Koronovskii, Alexey A. and Hramov, Alexander E. 2014 Higher harmonics generation in relativistic electron beam with virtual cathode. *Phys. Plasmas (1994-present)* **21**(9), 093105.
- Kurkin, S. A. and Hramov, A. E. 2009 Virtual cathode formation in annular electron beam in an external magnetic field. *Tech. Phys. Lett.* **35**(1), 23–25.
- Kurkin, S. A., Hramov, A. E. and Koronovskii, A. A. 2013 Microwave radiation power of relativistic electron beam with virtual cathode in the external magnetic field. *Appl. Phys. Lett.* **103**, 043507.
- Kurkin, S. A., Koronovskii, A. A. and Hramov, A. E. 2011 Output microwave radiation power of low-voltage vircator with external inhomogeneous magnetic field. *Tech. Phys. Lett.* **37**(4), 356–359.
- Liu, G., Shao, H., Yang, Z., Song, Z., Chen, C. H., Sun, J. and Zhang, Y. 2008 Coaxial cavity vircator with enhanced efficiency. *J. Plasma Phys.* **74**, 233–244.
- Mahaffey, R. A., Sprangle, P. A., Golden, J. and Kapetanakis, C. A. 1977 High-power microwaves from a non-isochronous reflecting electron system. *Phys. Rev. Lett.* **39**(13), 843.
- Morey, I. J. and Birdsall, C. K. 1990 Travelling-wave-tube simulation: the IBC code. *IEEE Trans. Plasma Sci.* **18**(3), 482.
- Moskalenko, O. I., Phrolov, N. S., Koronovskii, A. A. and Hramov, A. E. 2013 Synchronization in the network of chaotic microwave oscillators. *Eur. Phys. J. Spec. Top.* **222**, 2571–2582.
- Nation, J. A., Schachter, L., Mako, F. M., Len, L. K., Peter, W., Tang, C. M. and Srinivasan Rao, T. 2014 Advances in cold cathode physics and technology. *Proc. IEEE* **87**(5), 865–889.
- Phrolov, N. S., Koronovskii, A. A., Kalinin, Yu. A., Kurkin, S. A. and Hramov, A. E. 2014 The effect of an external signal on output microwave power of a low-voltage vircator. *Phys. Lett. A* **378**, 2423–2428.

- Rozhnev, A. G., Ryskin, N. M., Sokolov, D. V., Trubetskov, D. I., Han, S. T., Kim, J. I. and Park, G. S. 2002 Novel concepts of vacuum microelectronic microwave devices with field emitter cathode arrays. *Phys. Plasmas*. **9**(9), 4020–4027.
- Shao, H., Liu, G. and Yang, Z. 2005 Electron beam–electromagnetic field interaction in one-dimensional coaxial vircator. *J. Plasma Phys.* **71**(5), 563–578.
- Shlapakovski, A. S., Kweller, T., Hadas, Y., Krasik, Y. E., Polevin, S. D. and Kurkan, I. K. 2009 Effects of different cathode materials on submicrosecond double-gap vircator operation. *IEEE Trans. Plasma Sci.* **37**(7), 1233–1241.
- Shlapakovski, A. S., Queller, T., Bliokh, Yu. P. and Krasik, Y. E. 2012 Investigations of a double-gap vircator at sub-microsecond pulse durations. *IEEE Trans. Plasma Sci.* **40**(6), 1607–1617.
- Siegel, P. H., Fung, A., Manohara, H., Xu, J. and Chang, B. 2001 Nanoklystron: a monolithic tube approach to thz power generation. In: *Proc. 12th Int. Symp. on Space Terahertz Technology*, pp. 81–90.
- Stern, T. E., Gossling, B. S. and Fowler, R. H. 1929 Further studies in the emission of electrons from cold metals. *Proc. R. Soc. A* **124**(795), 699–723.
- Sullivan, D. J., Walsh, J. E. and Coutsiias, E. A. 1987 Virtual cathode oscillator (vircator) theory. *High Power Microwave Sources*, vol. 13 (ed. V. I. Granatstein and I. Alexeff). Norwood, MA: Artech House Microwave Library.
- Sze, H., Price, D., Harteneck, B. and Cooksey, N. 1990 A master-oscillator-driven phase-locked vircator array. *J. Appl. Phys.* **68**(7), 3073–3079.
- Verma, R. et al. 2014 Characterization of high power microwave radiation by an axially extracted vircator. *IEEE Trans. Electron Devices* **61**(1), 141–146.
- Woo, W., Benford, J., Fittinghoff, D., Harteneck, B., Price, D., Smith, R. and Sze, H. 1989 Phase locking of high-power microwave oscillator. *J. Appl. Phys.* **65**(2), 861.
- Yang, Z., Liu, G., Shao, H., Sun, J., Zhang, Y., Ye, H. and Yang, M. 2013 Numerical simulation study and preliminary experiments of a coaxial vircator with radial dual-cavity premodulation. *IEEE Trans. Plasma Sci.* **41**(12), 3604–3610.